Statistics of pressure and pressure gradient in homogeneous isotropic turbulence

By T. Gotoh[1] AND R. S. Rogallo[2]

The statistics of pressure and pressure gradient in stationary isotropic turbulence are measured within direct numerical simulations at low to moderate Reynolds numbers. It is found that the one-point pdf of the pressure is highly skewed and that the pdf of the pressure gradient is of stretched exponential form. The power spectrum of the pressure $P(k)$ is found to be larger than the corresponding spectrum $P_G(k)$ computed from a Gaussian velocity field having the same energy spectrum as that of the DNS field. The ratio $P(k)/P_G(k)$, a measure of the pressure-field intermittence, grows with wavenumber and Reynolds number as $-R_\lambda^{1/2}\log(k/k_d)$ for $k < k_d/2$ where k_d is the Kolmogorov wavenumber. The Lagrangian correlations of pressure gradient and velocity are compared and the Lagrangian time scale of the pressure gradient is observed to be much shorter than that of the velocity.

1. Introduction

The pressure field plays an important role in the turbulent motion of an incompressible fluid. The pressure, or more precisely its gradient, accelerates and deforms fluid blobs in a manner that prevents them from being compressed. The pressure is given by the solution of a Poisson equation, implying that it is a quantity dominated by the large scales of the velocity field, but the source term is quadratic in the velocity gradient and leads to non-Gaussian statistics of the pressure field. Recent studies have shown that the pdf of the pressure field is highly skewed and has a long tail for negative fluctuations. These fluctuations correspond to intense vortices with radii of the order of the Kolmogorov length (Holtzer & Siggia 1993, Pumir 1994).

The internal dynamics of a turbulent fluid motion can be extracted in a frame moving with the fluid (the Lagrangian point of view). At moderate to high Reynolds number, the pressure gradient rather than the viscous stress is responsible for the deformation and acceleration of fluid regions larger than the dissipation scale. For example the time scale of small scales of turbulent motion can be inferred from the curvature of the Lagrangian velocity auto-correlation obtained from the expansion

$$R_L(t,s) = \langle \mathbf{v}(t)\cdot\mathbf{v}(s)\rangle = C_0 - \frac{1}{2}C_2(t-s)^2 + \cdots, \qquad t \geq s, \tag{1.1}$$

1 Nagoya Institute of Technology, Japan
2 NASA Ames Research Center

$$C_0 = 2\int_0^\infty E(k,s)dk, \tag{1.2}$$

$$C_2 = -\langle(\nabla p(\mathbf{x},s))^2\rangle = -\int_0^\infty k^2 P(k,s)dk = -\int \frac{\langle D(\mathbf{k},s)D(-\mathbf{k},s)\rangle}{k^2}d\mathbf{k}, \tag{1.3}$$

$$D(\mathbf{k}) = k_i k_l \iint_{\mathbf{p}+\mathbf{q}=\mathbf{k}} d\mathbf{p}d\mathbf{q}\; u_i(\mathbf{p},s)u_l(\mathbf{q},s), \tag{1.4}$$

for small $t-s$. Here for simplicity we have neglected the viscous term and have taken $\rho = 1$. The power spectrum of the pressure $P(k,t)$ gives the pressure variance as

$$\langle p^2(\mathbf{x},t)\rangle = \int_0^\infty P(k,t)\; dk.$$

Eqs. (1.3) and (1.4) imply that the spectrum of the pressure gradient depends on a fourth-order moment of the velocity field, and roughly speaking the largest contribution to the pressure-gradient variance comes from wavenumbers lower than the peak wavenumber of $k^2E(k)$ when Reynolds number is large. This can be compared with the variance of the pressure itself, which is dominated by wavenumbers near the peak of the energy spectrum $E(k)$, and with the variance of the dissipation ϵ, which is dominated by wavenumbers near the peak of $k^2E(k)$.

It is well known that the small scales of turbulent motion are intermittent (we shall use this term herein to mean simply a departure from Gaussian statistics) and fourth-order moments have contributions from the cumulant part. An example is seen in Gotoh *et al* (1993) where the initial curvature $|C_2^{DNS}|$ is larger than $|C_2^G|$ computed from a Gaussian velocity field

$$\begin{aligned} C_2^G &= -\langle(\nabla p(\mathbf{x},s))^2\rangle_G = -\int_0^\infty k^2 P_G(k,s)dk \\ &= -\int_0^\infty dk \int_0^\infty dq\; kq\; J\left(\frac{q}{k}\right) E(k,s)E(q,s), \end{aligned} \tag{1.5}$$

$$J(x) = \{(a^2-1)^2 \log\frac{1+a}{|1-a|} - 2a + \frac{10}{3}a^3\}/(2a^4), \qquad a = \frac{2x}{1+x^2}. \tag{1.6}$$

This suggests that turbulence has a faster decay of $R_L(\tau)$ and a smaller turbulent diffusivity (as given by the time integral of $R_L(\tau)$) than predicted by the Gaussian theory. In other words, it suggests that the dynamics of the Navier-Stokes equation causes a fluid blob to forget its past history more effectively than would convection by a Gaussian velocity field. Therefore intermittence effects appear in the dynamics of a fluid particle through the pressure gradient and are expected to be different from those of the viscous stress, but we do not know how fast intermittence in the pressure increases with wavenumber, how it differs from the intermittence of the dissipation, what its time scale depends on, and so on.

There have been many studies of the fluctuations of pressure and its gradient in turbulence (Monin & Yaglom 1975, and Nelkin 1994) but few fundamental studies

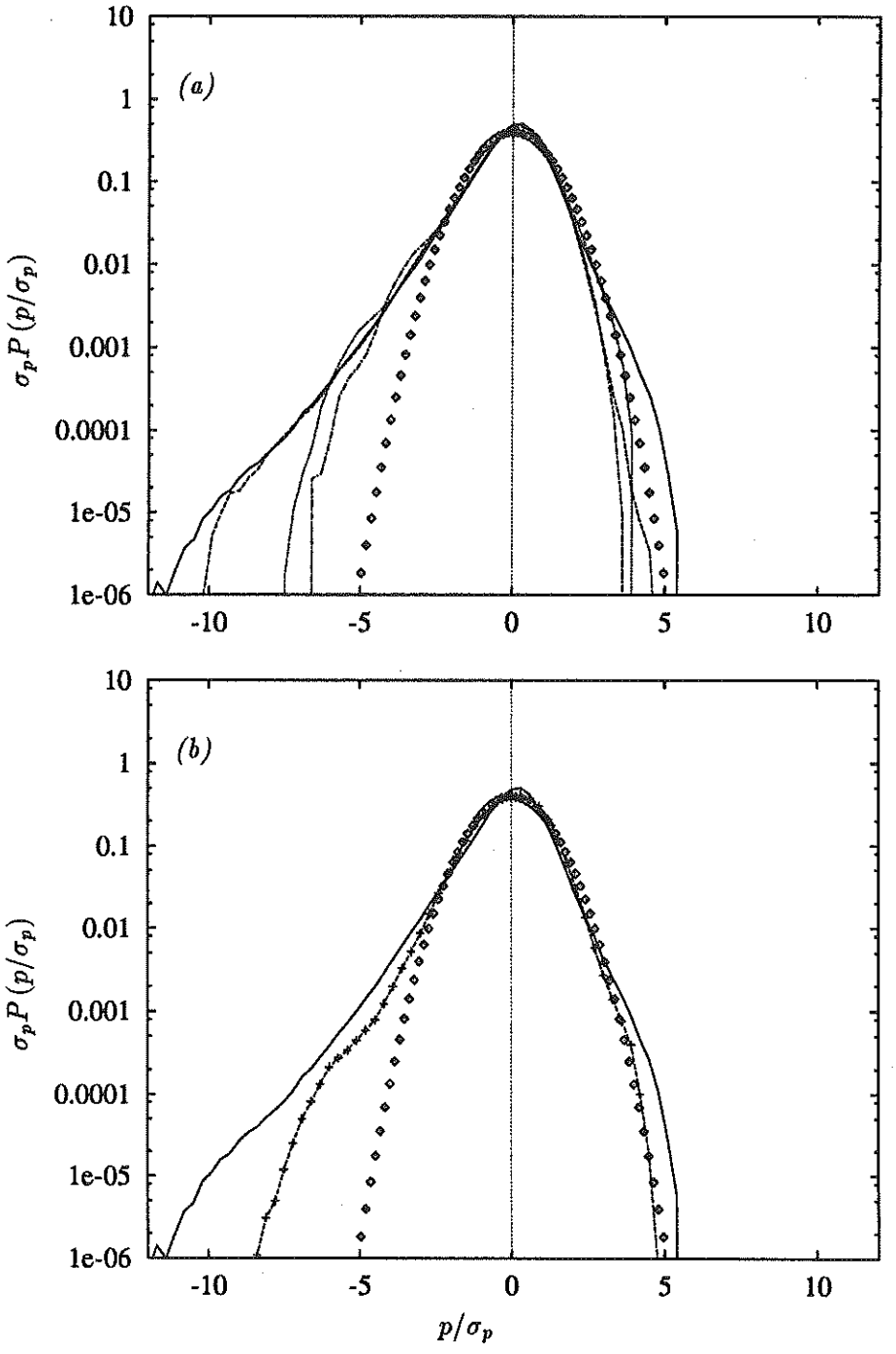

FIGURE 1. The pdf of pressure. (a) turbulent velocity field. ——— : $R_\lambda = 172$, - - - - : $R_\lambda = 96$, ····· : $R_\lambda = 63$, —·— : $R_\lambda = 38$, ◇: Gaussian, (b) Gaussian velocity field with the same energy spectrum for $R_\lambda = 172$. ——— : turbulent velocity field, +- - - - : Gaussian velocity field, ◇: Gaussian.

of pressure intermittence and its effects on the flow dynamics. This is partly because experimental measurement of the pressure spectrum is difficult (Uberoi 1953 and George *et al* 1984). Now that extensive numerical data are available, we can examine the statistics of the pressure field systematically, albeit at rather low Reynolds numbers. Here we present some measurements taken from the DNS data base available during the summer program and examine the statistics of the pressure field.

2. Numerical simulation

The turbulent flow fields used here (Jiménez *et al* 1993) are all homogeneous and isotropic and are held stationary by forcing at low wavenumber. They are arranged into four groups according to the Reynolds number R_λ, with statistical quantities computed as averages over two fields at well separated times for $R_\lambda = 172$ and over three fields for $R_\lambda = 96, 63, 38$. The numerical grid sizes were $N = 256^3$ for $R_\lambda = 172, 96$, $N = 128^3$ for $R_\lambda = 63$, and $N = 64^3$ for $R_\lambda = 38$. The Lagrangian autocorrelations of velocity and pressure gradient were computed by the passive-vector method (Kaneda & Gotoh 1991, Gotoh *et al* 1993). The pressure field $p(\mathbf{k}, t)$ was computed using de-aliased spectral methods.

3. Results

3.1. One-point one-time statistics

The one-point pdf of the pressure in Fig. 1a is skewed as reported by Pumir (1994). For negative pressure fluctuations the asymptotic form of the pdf tends to be nearly exponential $P(p) \propto \exp\left(-a|p/\sigma_p|^\alpha\right)$, where a is a non-dimensional constant and the exponent α is slightly less than one, which is consistent with low pressure in the core regions of intense vortex filaments. The tail of the pdf extends towards negative values with large amplitude as R_λ increases but α is independent of R_λ. For positive fluctuations the pdf is close to Gaussian and is insensitive to R_λ (Pumir 1994). Furthermore the pdf $P_G(p)$ of the pressure field computed from a Gaussian velocity field having the same energy spectrum has the same behavior (Fig. 1b) for the negative fluctuations as predicted by Holtzer & Siggia (1993).

The pdf of one component of the pressure gradient is shown in Fig. 2a for different Reynolds numbers. The pdf is symmetric and its tails become wider as R_λ increases. Fig. 2b shows that the pdf of the pressure gradient is isotropic and that it differs markedly from that computed from a Gaussian velocity field, unlike the case of the pressure itself. The asymptotic form of the tails of these pdf's appears to be a stretched exponential $P(p_{,i}) \propto \exp\left(-b\left|p_{,i}/\sigma_{p_{,i}}\right|^\beta\right)$ with $0 < \beta < 1$, where b is a non-dimensional constant, while that of its Gaussian counterpart is exponential as expected. This means that the pressure-gradient field is very intermittent and is quite different from the pressure gradient in a Gaussian velocity field. Holtzer & Siggia (1993) studied the pdf of the pressure gradient and suggested $\beta \sim 1/2$. The pdfs plotted against $\sqrt{p_{,y}/\sigma_{p_{,y}}}$ (figure not shown) indicate that β is close to 1/2 for large amplitudes and becomes smaller as R_λ increases.

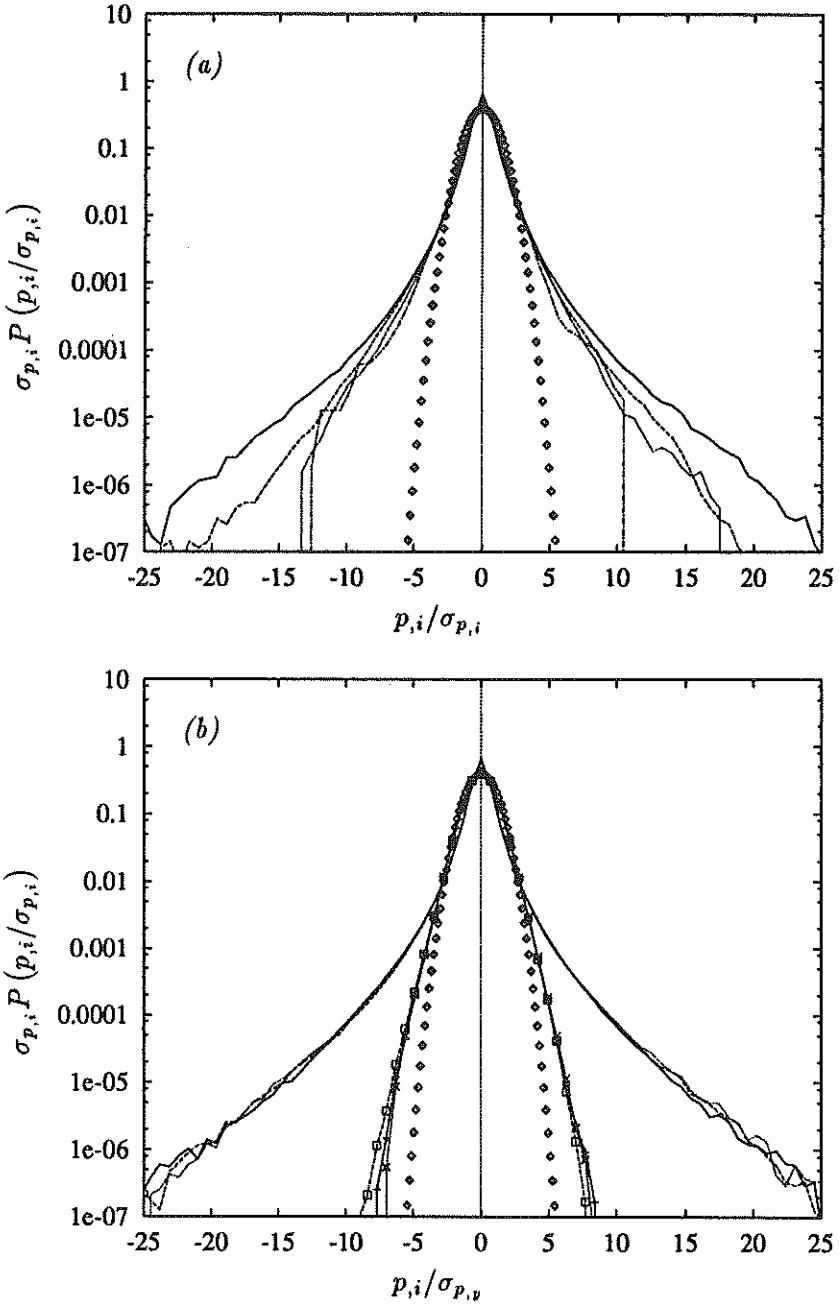

FIGURE 2. The pdf of pressure gradient. (a) variation with Reynolds number for a single component. ——— : $R_\lambda = 172$, - - - - : $R_\lambda = 96$, ····· : $R_\lambda = 63$, —·— : $R_\lambda = 38$, ◇: Gaussian, (b) Comparison of turbulent and Gaussian values for all components at $R_\lambda = 172$. ——— : $\partial p/\partial x$, - - - - : $\partial p/\partial y$, ····· : $\partial p/\partial z$ for turbulent velocity field; +——— : $\partial p/\partial x$, □- - - - : $\partial p/\partial y$, ×····· : $\partial p/\partial z$ Gaussian velocity field; ◇: Gaussian.

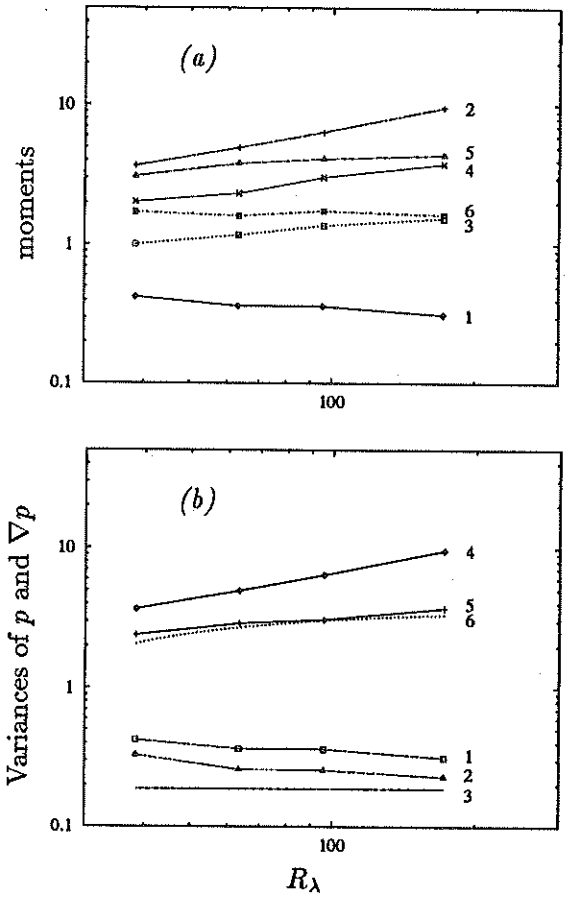

FIGURE 3. Variation with Reynolds number of velocity moments. (a) Various moments of turbulent velocity field. 1: F_p, 2: $F_{\nabla p}$, 3: F_ϵ, 4: F_ω, 5: $F_{\partial_1 u_1}$, 6: F_{u_1}. (b) Comparison with values from the corresponding Gaussian velocity fields. 1: F_p (DNS), 2: F_p (Gaussian), 3: F_p (George *et al* 1984), 4: $F_{\nabla p}(DNS)$, 5: $F_{\nabla p}$ (Gaussian), 6: $F_{\nabla p}$ (George *et al* 1984).

The variation with R_λ of normalized moments of the pressure and pressure gradient are shown in Fig. 3a. Included there for comparison are other normalized fourth-order moments of velocity:

$$F_p = \frac{\langle p^2 \rangle}{(\frac{1}{2}\langle \mathbf{u}^2 \rangle)^2}, \qquad F_{\nabla p} = \frac{\langle (\nabla p)^2 \rangle}{\bar{\epsilon}^{3/2}\nu^{-1/2}}, \tag{3.1}$$

$$F_\epsilon = \frac{\langle \epsilon^2 \rangle}{\langle \epsilon \rangle^2}, \quad F_\omega = \frac{\langle \omega^4 \rangle}{\langle \omega^2 \rangle^2}, \quad F_{\partial_1 u_1} = \frac{\langle (\partial u_1/\partial x_1)^4 \rangle}{\langle (\partial u_1/\partial x_1)^2 \rangle^2}, \quad F_{u_1} = \frac{\langle (u_1)^4 \rangle}{\langle (u_1)^2 \rangle^2}, \tag{3.2}$$

where $\bar{\epsilon} = \langle \epsilon \rangle$. The normalized variance of the pressure F_p is insensitive to R_λ (Batchelor 1951 and Pumir 1994). On the other hand the normalized variance of

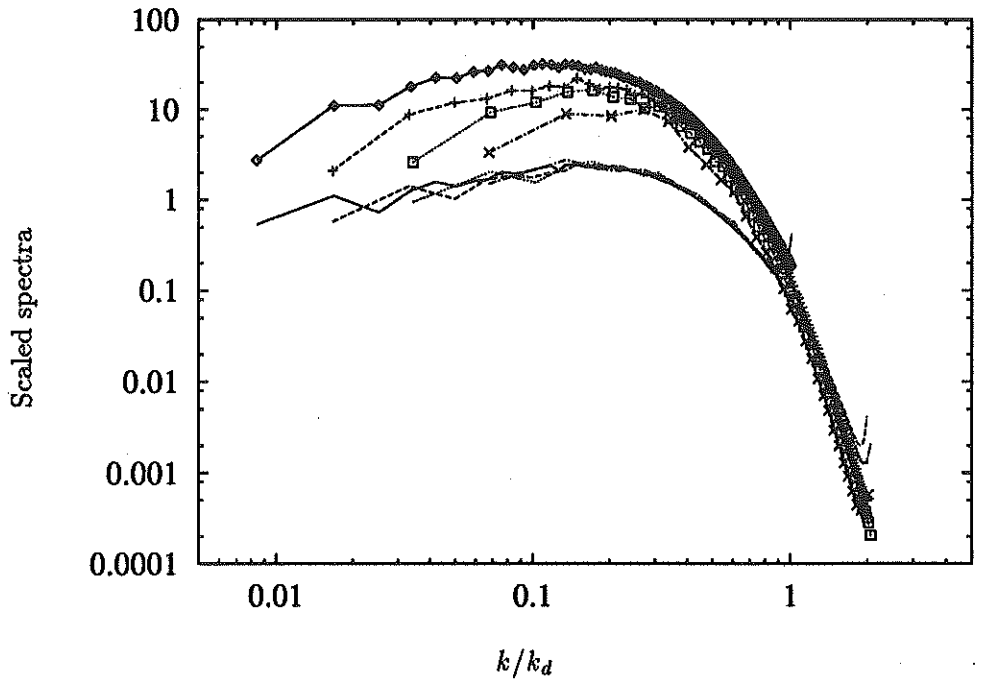

FIGURE 4. Velocity-gradient and pressure-gradient power spectra in Kolmogorov units. ——— : $R_\lambda = 172$, - - - - : $R_\lambda = 96$, ····· : $R_\lambda = 63$, —·— : $R_\lambda = 38$. Curves without symbols: $\bar{\epsilon}^{-3/4}\nu^{1/4}k^2E(k)$. Curves with symbols: $\bar{\epsilon}^{-5/4}\nu^{-1/4}k^2P(k)$.

the pressure gradient $F_{\nabla p}$ increases rapidly with R_λ and is roughly proportional to $R_\lambda^{1/2}$ for the range of Reynolds numbers studied here. This tendency is in agreement with Yeung & Pope (1989), where R_λ was below 93. On the other hand F_ϵ and F_ω increase slowly with R_λ in agreement with the data of Kerr (1985). This difference is surprising because functions of the velocity gradient such as vorticity or $\partial u_1/\partial x_1$ are quantities representing small scales of turbulent motion (characterized by wavenumbers near the maximum of $k^2E(k)$) and are believed to be more intermittent than the pressure-gradient field whose characteristic wavenumber is lower than that of $k^2E(k)$ when the Reynolds number is high (see Fig. 4).

When the universal equilibrium form of the energy spectrum (Kolmogorov 1941) is used with the Gaussian-velocity approximation (1.5) we obtain

$$\begin{aligned} E(k) &= \bar{\epsilon}^{1/4}\nu^{5/4}f(k/k_d), \\ \langle(\nabla p(\mathbf{x}))^2\rangle &= \bar{\epsilon}^{3/2}\nu^{-1/2}F_{\nabla p}, \\ F_{\nabla p} &= 2\int_0^\infty dx \int_0^x dy\; xy\; J\left(\frac{y}{x}\right) f(x)f(y), \end{aligned} \tag{3.3}$$

Kaneda (1993) analyzed (3.3) and found that the largest contribution to the integral comes from the region $y \le k_c/k_d \le x$, where k_c is the wavenumber above which

$E(x) \propto \exp(-cx)$ and c is a non-dimensional constant, which means that the integral $F_{\nabla p}$ is governed by the energy spectrum up to the dissipation range. Batchelor (1951) estimated $F_{\nabla p} \sim 3.9$ independent of R_λ. George *et al* (1984) used (3.3) with an empirical energy spectrum for $E(k)$ and found

$$F_{\nabla p} = \left(\beta_p - \frac{\gamma_p}{R_\lambda}\right), \tag{3.4}$$

with $\beta_p = 3.7$ and $\gamma_p = 62.7$. The constant β_p is universal while γ_p depends on the macro-scale of the turbulence.

Fig. 3b compares the variances of the pressure and its gradient with those computed from Gaussian velocity fields. The values computed from the Gaussian fields are close to those found from (3.4) using the values of George *et al* (1984) but are significantly lower than the DNS values. The R_λ dependence of the turbulent pressure gradient is stronger than that of its Gaussian counterpart, and it seems likely that any theoretical explanation must take into account the non-Gaussian statistics.

3.2. Two-point one-time statistics

Eqs. (1.3) and (1.4) show that the power spectrum of the pressure gradient is a function of a fourth-order moment of the velocity field. The Gaussian approximation for the velocity field leads to (1.5), which implies that the peak of $k^2P(k)$ occurs at a lower wavenumber than that of $k^2E(k)$. Comparison of these spectra, plotted in Kolmogorov units in Fig. 4, confirms that at low R_λ both spectra peak at nearly the same wavenumber, but as R_λ increases the peak of $k^2P(k)$ moves to lower wavenumber. Collapse of the enstrophy spectra is excellent but that of the pressure gradient is not. This implies that the Kolmogorov scaling is not appropriate for the pressure field (Moin & Yaglom 1975). The cumulative contributions of these spectra to the total enstrophy and pressure-gradient variance

$$Q_1(k) \equiv \frac{\int_0^k q^2 E(q)dq}{\int_0^{K_{max}} q^2 E(q)dq}, \quad Q_2(k) \equiv \frac{\int_0^k q^2 P(q)dq}{\int_0^{K_{max}} q^2 P(q)dq}, \tag{3.5a,b}$$

for the four R_λ's reach 80% at $k_p/k_d \approx 0.35$ for the pressure gradient and at $k_\omega/k_d \approx 0.5$ for total enstrophy, but their scale separation k_p/k_ω is small (Batchelor 1951).

One way to measure the variation of pressure intermittence across the spectrum is to compare the pressure power spectrum $P(k)$ of the turbulence with that $P_G(k)$ computed from a Gaussian velocity field (Hudong *et al* 1987). Fig. 5a presents such a comparison for $R_\lambda = 172$. The pressure spectrum $P(k)$ is larger than $P_G(k)$ for all wavenumbers beyond the forced range, meaning that the cumulant contribution $P_C(k)$,

$$P(k) = P_G(k) + P_C(k), \tag{3.6}$$

is positive. This suggests that the inertial-range constant K_p for the pressure spectrum $P(k) = K_p\bar{\epsilon}^{4/3}k^{-7/3}$ is larger than that predicted from the Gaussian velocity

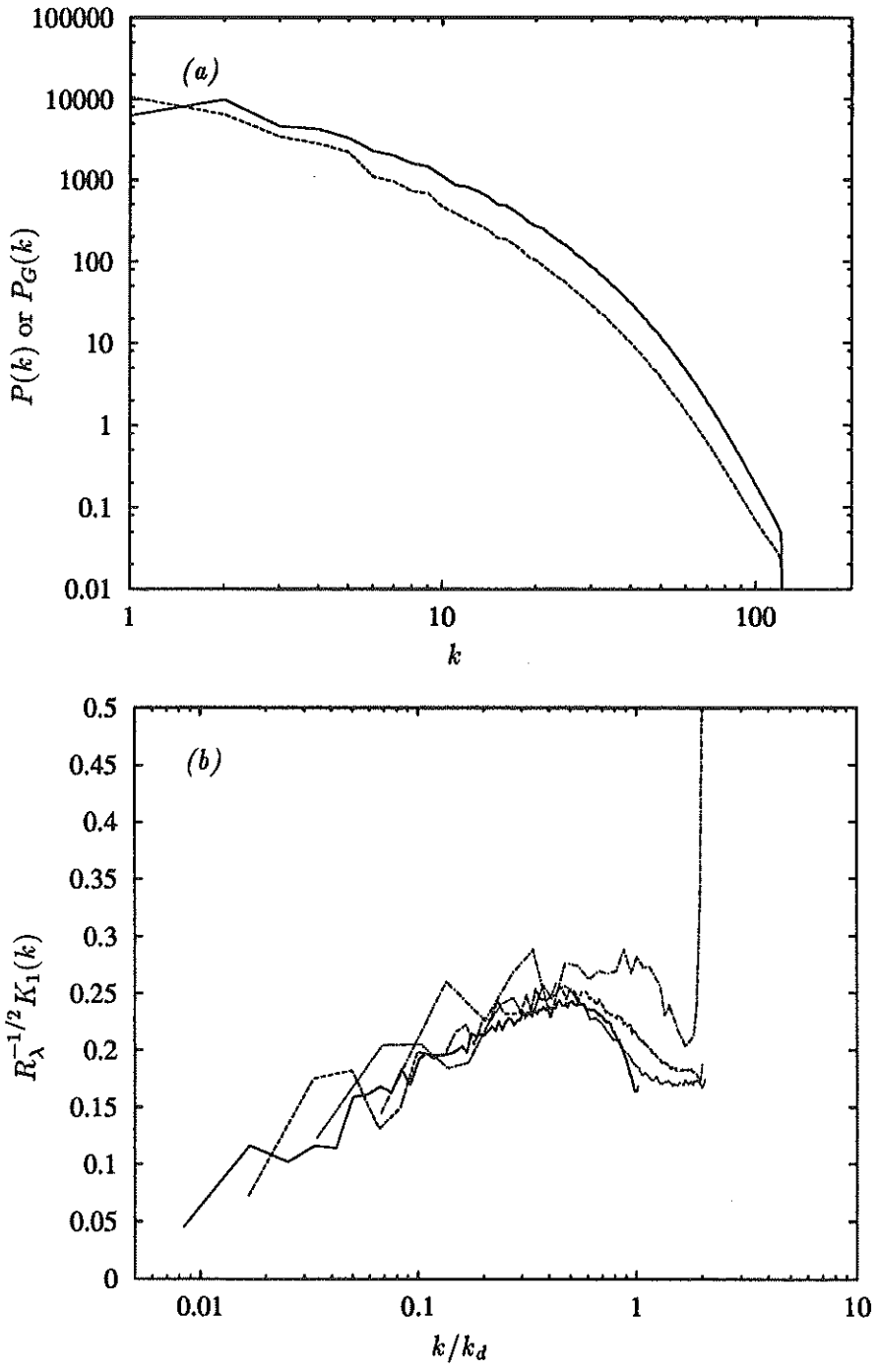

FIGURE 5. Comparison of pressure power spectra in turbulence with those computed from Gaussian velocity fields. (a) at $R_\lambda = 172$. ——— : $P(k)$, - - - - : $P_G(k)$. (b) variation of their (scaled) ratio $R_\lambda^{-1/2} K_1(k)$ with Reynolds number. ——— : $R_\lambda = 172$, - - - - : $R_\lambda = 96$, ····· : $R_\lambda = 63$, —·— : $R_\lambda = 38$.

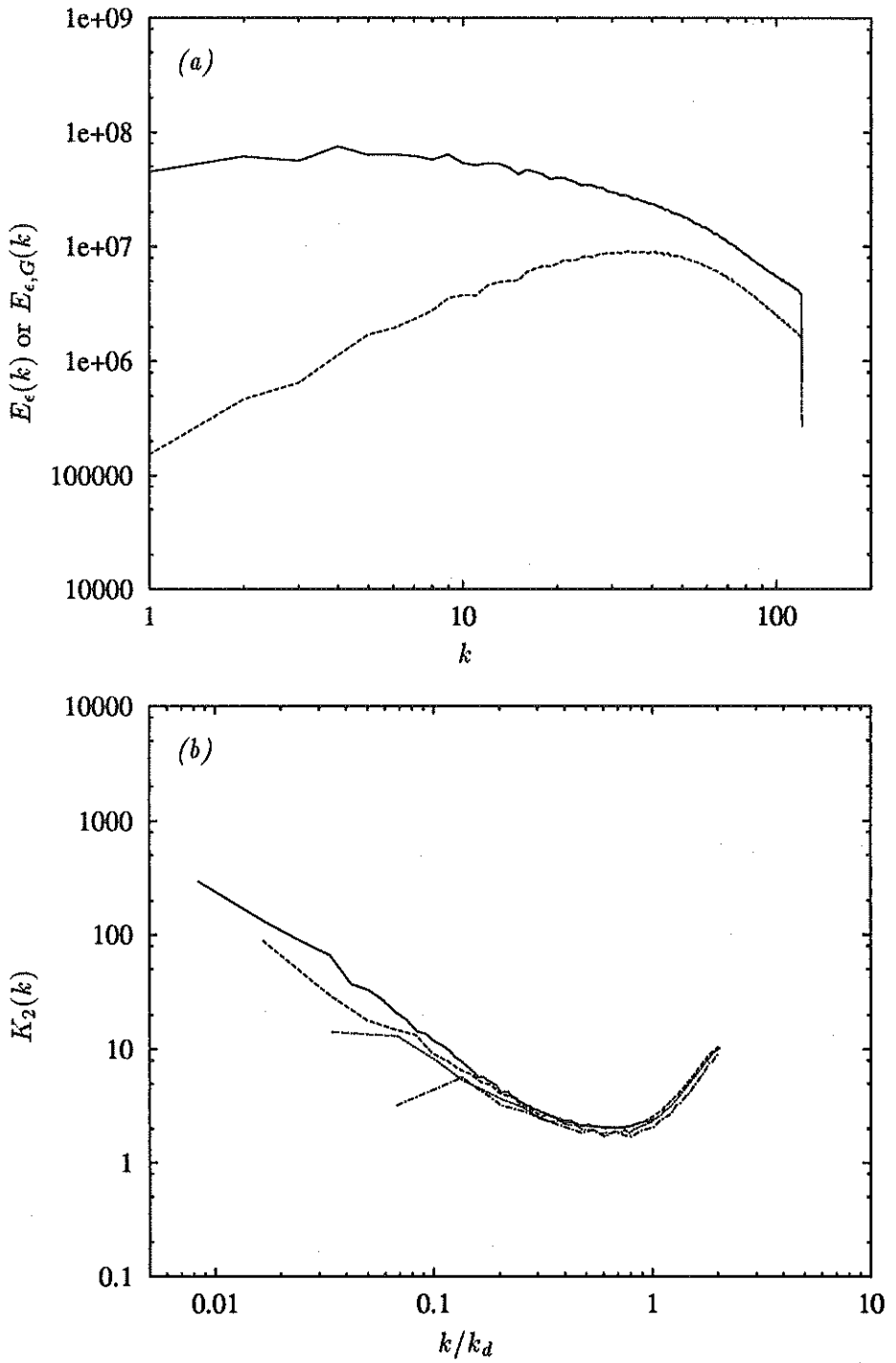

FIGURE 6. Comparison of dissipation power spectra in turbulence with those computed from Gaussian velocity fields. (a) at $R_\lambda = 172$. ——— : $E_\epsilon(k)$, - - - - : $E_{\epsilon,G}(k)$. (b) variation of their ratio $K_2(k)$ with Reynolds number. ———: $R_\lambda = 172$, - - - - : $R_\lambda = 96$, ····· : $R_\lambda = 63$, —·— : $R_\lambda = 38$.

field (Nelkin & Tabor 1990, Fung *et al* 1992, and the article by Pullin & Rogallo in this proceedings). We consider the spectrum ratio

$$K_1(k) = \frac{P(k)}{P_G(k)} \tag{3.7}$$

as a measure of the variation of pressure (and pressure gradient) intermittence across the spectrum. A $R_\lambda^{1/2}$ dependence of $K_1(k)$ is suggested by the good collapse of $R_\lambda^{-1/2} K_1(k)$ shown in Fig. 5b. This implies that

$$K_1(k) = 1 + \frac{P_C(k)}{P_G(k)} \propto -R_\lambda^{1/2} \log\left(\frac{k}{k_d}\right), \qquad k/k_d \leq 1/2. \tag{3.8}$$

The growth with wavenumber of the intermittence of second-order moments of the pressure field is very slow (it appears to be logarithmic, but the scale range is not sufficient to preclude a weak algebraic dependence) but the growth with Reynolds number as $R_\lambda^{1/2}$ is faster than that of other small-scale quantities. At $R_\lambda = 172$

$$\frac{\langle (\nabla p)^2 \rangle}{\langle (\nabla p)^2 \rangle_G} = 2.58 \tag{3.9}$$

and the initial curvature of the Lagrangian velocity autocorrelation is larger than that of the Gaussian field (Gotoh *et al* 1993). Navier-Stokes dynamics decorrelates the velocity of fluid particles faster than convection by a Gaussian velocity field would.

The variation of the dissipation intermittence across the spectrum is measured in a similar way. Fig. 6 compares the dissipation power spectra of turbulent-velocity fields with those of the corresponding Gaussian-velocity fields. Here we define the power spectrum of the dissipation and its intermittence (ratio of turbulent to Gaussian spectra) as

$$\langle \epsilon^2(\mathbf{x}, t) \rangle = \int_0^\infty E_\epsilon(k, t)\, dk, \tag{3.10}$$

$$K_2(k) = \frac{E_\epsilon(k)}{E_{\epsilon,G}(k)}. \tag{3.11}$$

The intermittence within the dissipation range is independent of Reynolds number. It is interesting to note that the maxima of $K_1(k)$ and minima of $K_2(k)$ both occur at $k/k_d \approx 1/2$ and that the diameter of intense vortex tubes is also of order $1/k_d$ (Jiménez *et al* 1993). The strong variation of the dissipation intermittence across the spectrum is opposite to that of the pressure field due to the modulation of the energy spectrum by the small-scale structures (Hudong *et al* 1987). For example when strong singularities of the velocity field with support size $1/k_d$ are placed periodically at a fixed separation $l \gg 1/k_d$, the power spectrum of the dissipation field has an excitation at $k \sim 1/l \ll k_d$ as well as at $k \sim k_d$, while a Gaussian velocity field with a compact spectrum centered on k_d simply generates a compact dissipation spectrum centered on k_d.

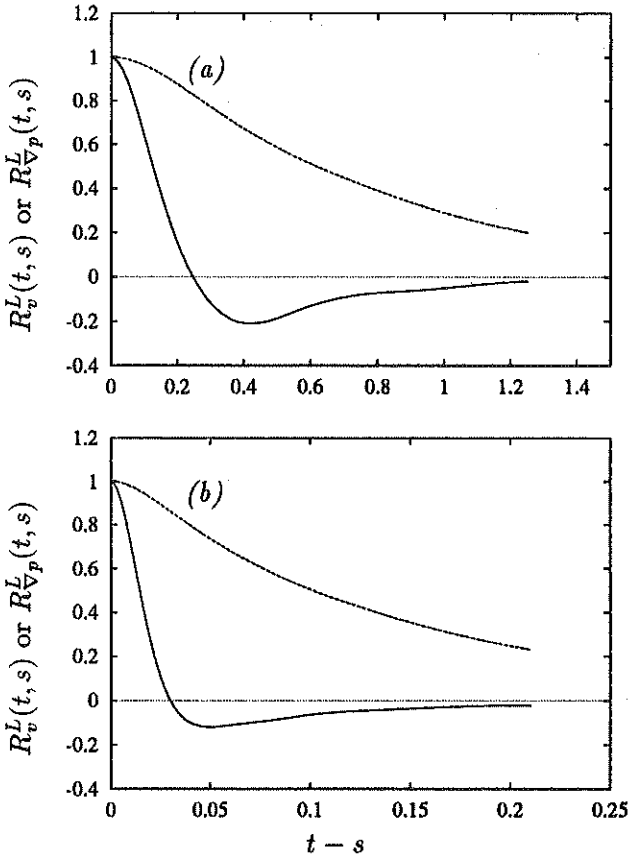

FIGURE 7. Lagrangian correlations of velocity and pressure gradient. (a) $R_\lambda = 63$. (b) $R_\lambda = 96$. ——— : $R_{\nabla p}^L(t,s)$, ---- : $R_v^L(t,s)$.

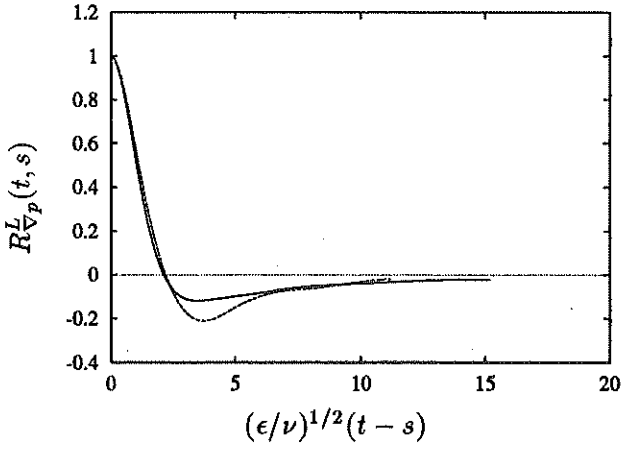

FIGURE 8. Kolmogorov time-scaling of the Lagrangian pressure-gradient correlation. ——— : $R_\lambda = 96$, ---- : $R_\lambda = 63$.

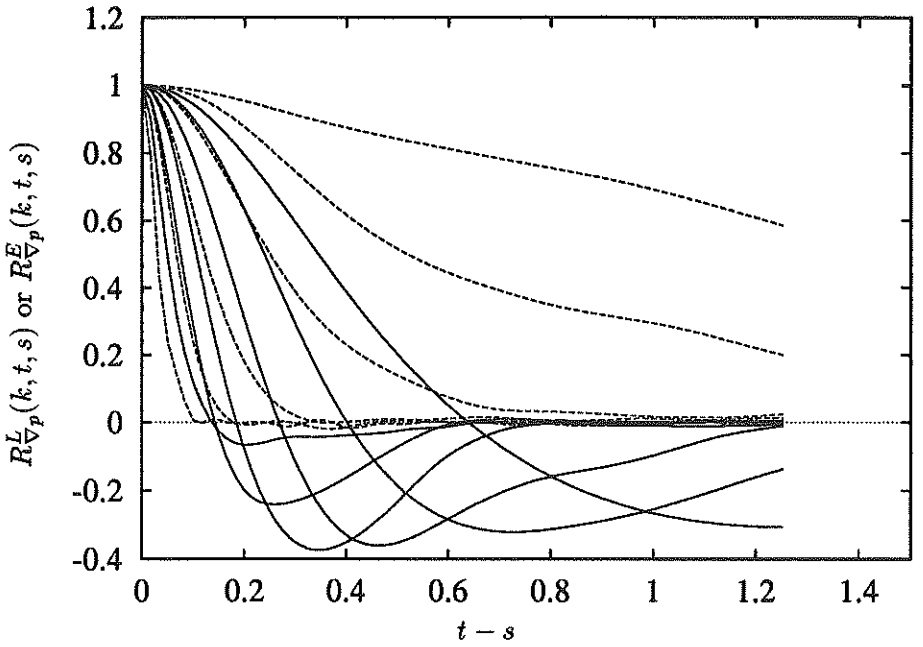

FIGURE 9. The decay of Lagrangian and Eulerian pressure-gradient correlations within octave bands at $R_\lambda = 63$. ——— : Lagrangian, ---- : Eulerian. The uppermost curves correspond to the lowest octaves and the correlations decrease monotonically for higher octaves.

9.3. Two-time statistics

The normalized Lagrangian auto-correlations of velocity and pressure gradient are defined in a stationary flow as

$$R^L_v(t,s) = \frac{\langle \mathbf{v}(\mathbf{x},t|t)\cdot\mathbf{v}(\mathbf{x},t|s)\rangle}{\langle|\mathbf{v}(\mathbf{x},s|s)|^2\rangle}, \qquad \text{for } t \geq s, \tag{3.12a}$$

$$R^L_{\nabla p}(t,s) = \frac{\langle \mathbf{F}(\mathbf{x},t|t)\cdot\mathbf{F}(\mathbf{x},t|s)\rangle}{\langle|\mathbf{F}(\mathbf{x},s|s)|^2\rangle}, \qquad \text{for } t \geq s, \tag{3.12b}$$

where $\mathbf{v}(\mathbf{x},t|s)$ is the velocity at time s of the fluid particle whose space-time trajectory passes through $(\mathbf{x},t)$, and $\mathbf{F}(\mathbf{x},t|s)$ is the pressure gradient acting on that particle at time s. Note that $\mathbf{v}(\mathbf{x},t|t) = \mathbf{u}(\mathbf{x},t)$ and $\mathbf{F}(\mathbf{x},t|t) = \nabla p(\mathbf{x},t)$.

Fig. 7 compares the Lagrangian auto-correlations $R^L_v(t,s)$ and $R^L_{\nabla p}(t,s)$ at $R_\lambda = 63$ and 96. The correlations of the pressure gradient decay much faster than those of the velocity and have negative correlation at later times. In Fig. 8 $R^L_{\nabla p}(t,s)$ is replotted with time scaled in Kolmogorov units. Collapse of the curves is excellent up to the time at which they change sign.

We define octave-band Lagrangian correlation spectra for the pressure gradient

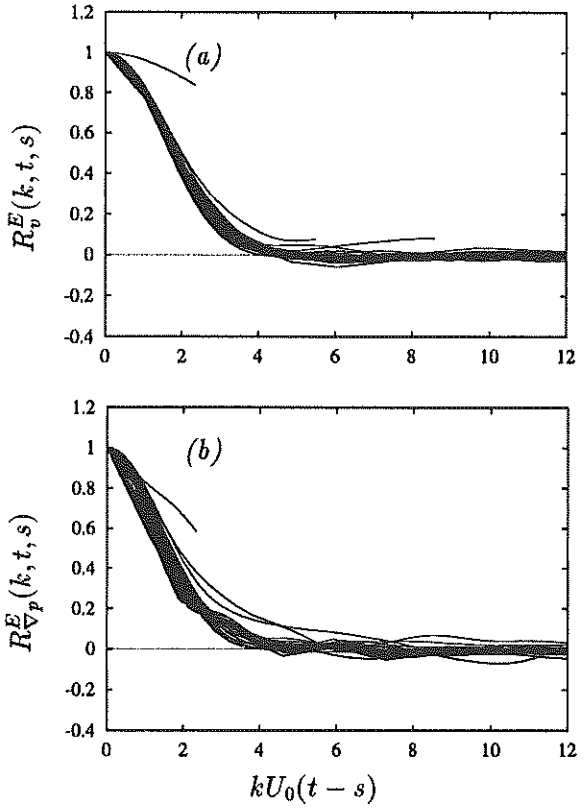

FIGURE 10. Time-scaled narrow-band Eulerian correlations of velocity and pressure gradient for wavenumber-bands $k = 2 + 2n, n = 0, \cdots 29$ at $R_\lambda = 63$. (a) $R_v^E(k,t,s)$. (b) $R_{\nabla p}^E(k,t,s)$.

as

$$\widehat{R}_{\nabla p}^L(k,t,s) = \frac{\sum_{oct} \langle \mathbf{F}(\mathbf{k},t|t) \cdot \mathbf{F}(-\mathbf{k},t|s) \rangle}{\left[\sum_{oct} |\mathbf{F}(\mathbf{k},t|t)|^2 \sum_{oct} |\mathbf{F}(\mathbf{k},t|s)|^2 \right]^{1/2}}, \tag{3.13}$$

where $\sum_{oct} \equiv \sum_{k=2^l}^{k=2^{l+1}}$ and $\mathbf{F}(\mathbf{k},t|s)$ is the Fourier transform of $\mathbf{F}(\mathbf{x},t|s)$ with respect to the *Lagrangian coordinates* at *labeling time* t (Kraichnan 1966 and Gotoh *et al* 1993). The octave-band Eulerian correlations are defined in a similar way.

The comparison of these spectra in Fig. 9 indicates that at high wavenumbers the Lagrangian correlation decays slower than the Eulerian, but that at low wavenumbers the decay rates are roughly equal. The Eulerian decorrelation of the small scales is caused primarily by their sweeping by larger scales while their Lagrangian decorrelation is due to deformation by larger scales. The sweeping effect on the Eulerian correlation is clearly demonstrated in Fig. 10 where narrow-band Eulerian correlation spectra, defined similarly to (3.13) with $\sum_{oct}$ replaced by $\sum_{shell}$, are

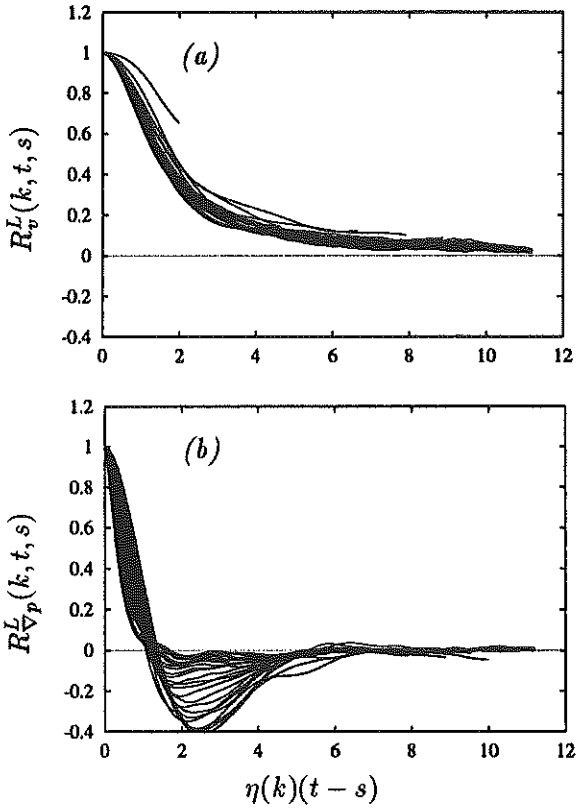

FIGURE 11. Time-scaled narrow-band Lagrangian correlations of velocity and pressure gradient for wavenumber-bands $k = 2 + 2n, n = 0, \cdots 29$ at $R_\lambda = 63$. (a) $R_v^L(k,t,s)$. (b) $R_{\nabla p}^L(k,t,s)$. The low-wavenumber bands display pronounced negative values.

plotted against the normalized time $kU_0(t-s)$. On the other hand, in Fig. 11, the narrow-band Lagrangian correlation spectra collapse when plotted against the normalized time $\eta(k)(t-s)$, where

$$\eta(k) = \left(\int_0^k q^2 E(q)\, dq \right)^{1/2} \tag{3.14}$$

is the rms strain rate of eddies larger than $1/k$ (the inverse of the turnover time for an eddy of that size), which is obtained from (1.5) by using the expansion of $J(x) \sim \frac{16\pi}{15} x$ for small x (Gotoh *et al* 1993). The success of these scalings is confirmed by a comparison of Figs. 10b and 11b with the unscaled data in Fig. 9.

4. Conclusions

Pressure statistics have been examined within a DNS of stationary isotropic turbulence. The one-point pdf of the pressure has an exponential tail for negative

fluctuations while that of the pressure gradient is symmetric and of stretched exponential form. The normalized variance of the pressure is insensitive to R_λ but the normalized variance of the pressure gradient increases as $R_\lambda^{1/2}$. The variances of both pressure and its gradient in the DNS are higher than those computed from a Gaussian field having the same energy spectrum.

The growth of intermittence across the pressure spectrum, characterized by the ratio of power spectra $P(k)/P_G(k)$, was found to be proportional to $-R_\lambda^{1/2}\log(k/k_d)$ for $k/k_d < 1/2$. The Lagrangian pressure-gradient correlation has a time scale much shorter than that of the velocity and its narrow-band spectra change sign at the normalized time $\eta(k)(t-s) \approx 1$. This is consistent with the notion of a fluid particle being accelerated toward the center of a vortex of size $1/k$ by the pressure gradient acting on that particle.

Previous theoretical analyses of these observations are rather scarce (Pullin 1994 and Nelkin 1994) due to the difficulty of dealing with the nonlocality in physical space of the Poisson equation for the pressure field. Most studies so far are based on the Gaussian velocity approximation, but intermittence effects in the pressure field are clearly evident in its one-point statistics as well as its spectrum. The construction of a theory that is able to explain these observations is a real challenge.

Acknowlegements

The authors have benefited from fruitful discussions with Profs. D. Pullin, Y. Kaneda, and Dr. R. H. Kraichnan. TG also expresses his thanks for partial support from the Tatematsu and the Daiko foundations.

REFERENCES

BATCHELOR, G. K. 1951 Pressure fluctuations in isotropic turbulence. *Proc. Camb. Phil. Soc.* **47**, 359-374.

FUNG, J. C. H., HUNT, J. C. R., MALIK, N. A., & PERKINS, R. J. 1992 Kinematic simulation of homogeneous turbulence by unsteady random Fourier modes. *J. Fluid Mech.* **236**, 281-318.

GOTOH, T., ROGALLO, R. S., HERRING, J. R., & KRAICHNAN, R. H. 1993 Lagrangian velocity correlations in homogeneous isotropic turbulence. *Phys. Fluids A.* **5**, 2846-2864.

GEORGE, W., BEUTHER, P. D., & ARNDT, R. E. 1984 Pressure spectra in turbulent free shear flows. *J. Fluid Mech.* **148**, 155-191.

HOLTZER, M. & SIGGIA, E. 1993 Skewed, exponential pressure distributions from Gaussian velocities. *Phys. Fluids A.* **5**, 2525-2532.

HUDONG, C., HERRING, J. R., KERR, R. M., & KRAICHNAN, R. H. 1987 Non-Gaussian statistics in isotropic turbulence. *Phys. Fluids A.* **1**, 1844-1854.

JIMÉNEZ, J., WRAY, A. A., SAFFMAN, P. G., & ROGALLO, R. S. 1993 The structure of intense vorticity in isotropic turbulence. *J. Fluid Mech.* **255**, 65-90.

KANEDA, Y. 1993 Lagrangian and Eulerian time correlations in turbulence. *Phys. Fluids A.* **5**, 2835-2845.

KANEDA, Y. & GOTOH, T. 1991 Lagrangian velocity autocorrelation in isotropic turbulence. *Phys. Fluids A.* **3**, 1924-1933.

KERR, R. M. 1985 High-order derivative correlations and the alignment of small-scale structures in isotropic numerical turbulence. *J. Fluid Mech.* **153**, 31-58.

KRAICHNAN, R. H. 1966 Isotropic turbulence and inertial-range structure. *Phys. Fluids.* **9**, 1728-1752.

MONIN, A. S. & YAGLOM, A. M. 1975 *Statistical Fluid Mechanics, Mechanics of Turbulence, Vol. 2.* MIT press.

NELKIN, M. 1994 Universality and scaling in fully developed turbulence. *Advances in Physics* (preprint).

NELKIN, M. & TABOR, M. 1990 Time correlations and random sweeping in isotropic turbulence. *Phys. Fluids A.* **2**, 81-83.

PULLIN, D. I. 1994 Pressure spectra for vortex models of fine-scale homogenous turbulence (preprint).

PUMIR, A. 1994 A numerical study of pressure fluctuations in three-dimensional, incompressible, homogeneous, isotropic turbulence. *Phys. Fluids.* **6**, 2071-2083.

UBEROI, M. S. 1953 Quadruple velocity correlations and pressure fluctuations in isotropic turbulence. *J. Aero. Sci.* **20**, 197-204.

YEUNG, P. K. & POPE, S. B. 1989 Lagrangian statistics from direct numerical simulations of isotropic turbulence. *J. Fluid Mech.* **207**, 531-586.